regarding this research and this manuscript.

References

Adams, D. K. and A. Comrie, 1997: The North American Monsoon. *Bull. Amer. Meteor. Soc*., **78**, 2197-2213.

Gochis, D.J., A. Jimenez, C.J. Watts, W.J. Shuttleworth, J. Garatuza-Payan,, 2004: Analysis of 2002 and 2003 warm-season precipitation from the North American Monsoon Experiment event rain gauge network. *Mon. Wea. Review*, **132**, 2938-2953.

Higgins, R.W. D. Ahijevych, J. Amador, A. Barros, E.H. Berbery, E. Caetano, R. Carbone, P. Ciesielski, R. Cifelli, M. Cortez-Vazquez, A. Douglas, M. Douglas, G. Emmanuel, C. Fairall, D. Gochis, D. Gutzler, T. Jackson, R. Johnson, C. King, T. Lang, M.I. Lee, D. Lettenmaier, R. Lobato, V. Magaña, J. Meiten, K. Mo, S. Nesbitt, F. Ocampo-Torres, E. Pytlak, P. Rogers, S. Rutledge, J. Schemm, S. Schubert, A. White, C. Williams, A. Wood, R. Zamora, and C. Zhang, 2006: The North American Monsoon Experiment (NAME) 2004 field campaign and modeling strategy. *Bull. Amer. Meteor. Soc*., **87**(1), 79-94.

Kursinski, A. L., and S. L. Mullen, 2008: Spatiotemporal variability of hourly precipitation over the Eastern Contiguous United States from Stage IV multisensor analyses, *Journal of Hydrometeorology*, **9**, 3–21.

Kursinski, E.R., R. A. Bennett, D. Gochis, S. I. Gutman, K. L. Holub, R. Mastaler, C. Minjarez Sosa, I. Minjarez Sosa, and T. van Hove, 2008: Water vapor and surface observations in northwestern Mexico during the 2004 NAME Enhanced Observing Period, *Geophys. Res. Lett*., **35**.

Lee, M.I., S.D. Schubert, M.J. Suarez, I.M. Held, A. Kumar, T.L. Bell, J.K.E. Schemm, N.C. Lau, J.J. Ploshay, H.K. Kim, and S.H. Yoo, 2007: Sensitivity to horizontal resolution in the AGCM simulations of warm season diurnal cycle of Precipitation over the United States and Northern Mexico. *J. Climate*, **20**, 1862–1881.

Weckwerth T. M., D. B. Parsons, S. E. Koch, J. A. Moore, M. A. Lemone, B. B. Demoz, C. Flamant, B. Geerts, J. Wang, and W. F. Feltz, 2004: An overview of the international H2O project (IHOP 2002) and some preliminary highlights, *Bull. Amer. Meteor Soc.*, **85**,253-277 DOI: 10.1175/BAMS-85-2-253.

Relation between surface flux measurements and hydrologic conditions in a subtropical scrubland during the North American Monsoon

Vivoni, E.R[1]., C.J. Watts[2], J.C. Rodríguez[2], J. Garatuza-Payan[3], L.A. Méndez-Barroso[1], E.A. Yepez[4], J. Saiz-Hernández[2],and D.J. Gochis[5]
[1]Department of Earth and Environmental Science, New Mexico Institute of Mining and Technology, [2]Departamento de Física, Universidad de Sonora, México. [3]Departamento de Ciencias del Agua y del Medioambiente, Instituto Tecnológico de Sonora, México. [4]Department of Biology, University of New Mexico, [5]. National Center for Atmospheric Research, USA.
Corresponding author: vivoni@nmt.edu.

Introduction

The North American monsoon (NAM) is the primary climatological phenomenon in the southwestern United States and northwestern Mexico, leading to large changes in precipitation, atmospheric conditions, vegetation and overall land surface properties (e.g., Douglas et al., 1993). Previous studies carried out by the North American Monsoon Experiment (NAME) have focused on the relationship and potential feedbacks between the NAM and the conditions of the land surface, including changes in vegetation, soil moisture and streamflow (Zhu et al., 2005; Gochis et al., 2006; Watts et al., 2007; Vivoni et al., 2007). Evidence from these studies suggests dramatic transitions in the hydrological conditions of the region. For example, in the seasonal march of the runoff ratio (Gochis et al., 2006) and in sharp changes in the surface fluxes (Watts et al., 2007). Here, we present multiple-year evidence for the relation between surface flux measurements and hydrologic conditions in a subtropical scrubland, one of the major regional ecosystems, which experiences significant greening during the NAM (Salinas-Zavala et al., 2002; Watts et al., 2007). The analysis is based on measurements at and around an Eddy Covariance (EC) tower located in Rayón, Sonora, Mexico within the Río San Miguel river (~3500 km^2) basin.

Surface Flux Measurements

Recent land-atmosphere interaction studies in the NAM region have focused on understanding the impact of vegetation greening on the measurement of soil moisture and energy balance components, including evapotranspiration. While these efforts began during the NAME 2004 campaign, subsequent studies have been sponsored by NSF, CONACYT and NOAA. Our focus is on the relation of surface fluxes, soil moisture and land surface conditions at the Rayón EC site (denoted as STS in Watts et al., 2007). The site is located at ~630 m in the Río San Miguel, a large ephemeral river basin, flowing north to south in the northern Sierra Madre Occidental. Vegetation at the site is classified as subtropical scrubland and is a mixture of trees, shrubs and desert cactus that respond to the precipitation pulses during the NAM. Soil profiles in the region are shallow (~70 cm in depth above an impermeable clay lens) and primarily composed of loamy sand and sandy loam with intermixed clasts.

Figure 1a (page 22) illustrates the experimental design for surface fluxes and footprint measurements of soil moisture and temperature. The footprint of the EC tower is defined here as a 250-m by 250-m region around the site, selected based on the pixel dimensions of the MODIS sensor. Within the EC tower footprint (see below), 30 sampling plots were established to relate these land surface conditions to the surface flux measurements. The 9-m tower contains a 3D sonic anemometer, as well as high frequency measurements of air temperature and relative humidity to estimate the covariance terms necessary to obtain the latent and sensible heat fluxes (Watts et al., 2007). Hydrometeorological observations at the site also include precipitation, soil moisture and temperature (at three depths), and radiation components used to estimate albedo and net radiation. Operation of the Rayón EC site has concentrated on summer campaign periods in 2004, 2006 and 2007, in particular to capture the changing conditions during the NAM onset, peak and demise (e.g. vegetation greening, see Figure 1b, c).

In Figure 2 (page 16), we present a comparison of remotely-sensed and field observations of rainfall, surface fluxes and land surface conditions during three monsoon periods (2004, 2006, 2007) at the EC tower site. Several interesting transitions are observed in vegetation cover, surface albedo and surface fluxes during the NAM, as well as important differences among the monsoon seasons. Vegetation dynamics are captured by the Normalized Difference Vegetation Index (*NDVI*) estimated at the tower pixel (250-m by 250-m) from 16-day MODIS composites. Vegetation dynamics are clearly tied to the daily precipitation, with early or late monsoon greening tightly related to the onset of precipitation. Similarly, the decrease in *NDVI* during the monsoon demise is tied to the available precipitation in the late summer. It is interesting to compare,

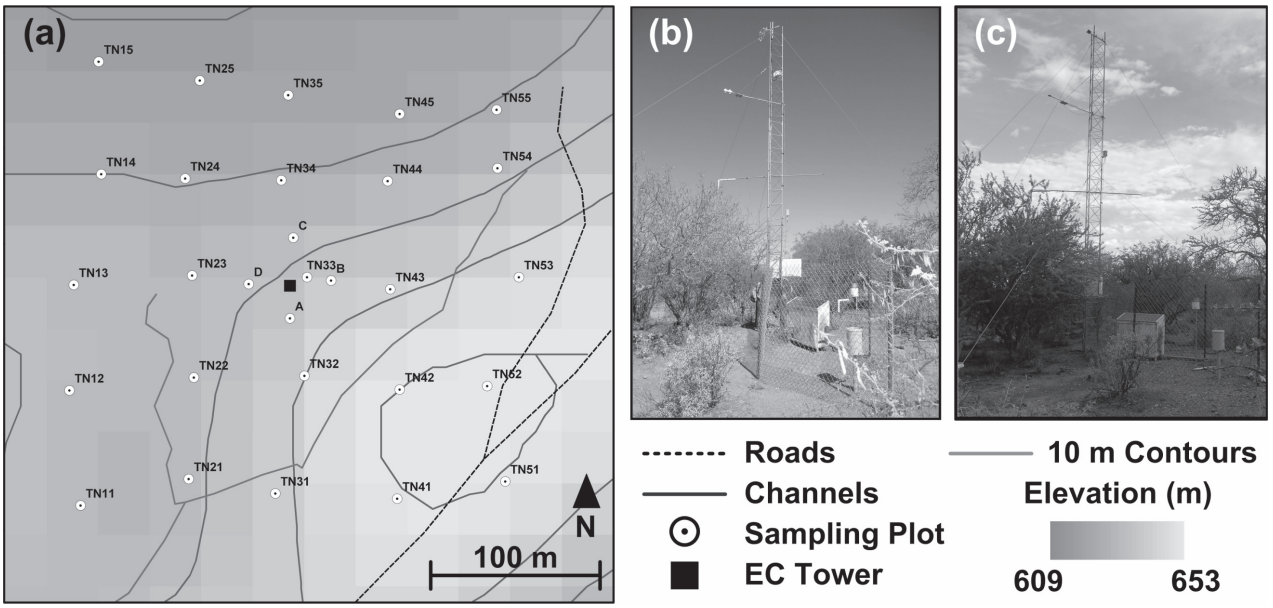

Figure 1. EC tower location and footprint sampling plots in Rayón, Sonora (30.04°N, 110.67°W). (a) Thirty sampling plots (white circles) in a 250-m box surrounding tower site (black square) overlain on a 30-m DEM (Digital Elevation Model) derived from ASTER (Advanced Spaceborne Thermal Emission and Reflection Radiometer). Roads and channels were traced using a GPS. (b) and (c) are photographs of the EC tower taken during a June period prior to the monsoon onset and a July period after monsoon greening, respectively.

for example, monsoon 2006 (Figure 2b) with a high peak *NDVI* and early onset, with monsoon 2007 (Figure 2c), which showed a reduced *NDVI* peak, a later onset but longer duration.

Vegetation greening is closely tied to the changes in albedo observed at the site from two sources: MODIS 16-day broadband albedo composites (1-km resolution) and EC tower albedo estimates. Comparison between the two albedo estimates is remarkably good, given the differences is spatial resolution (1 km^2 versus ~4 m^2 field of view), suggesting a spatially coherent change in vegetation cover in the vicinity of the tower. The clearest transition in albedo is observed for monsoon 2007 (Figure 2c) which spans the largest time period. Note that the vegetation greening indicated by increasing *NDVI* is coincident with the decrease in albedo. As expected, the land surface greening decreases the surface albedo, although the change is not very large (from ~0.18 to ~0.15), possibly due to the low leaf area and the extensive bare ground in this ecosystem. Given the high amounts of incoming solar radiation at the site, however, even small changes in albedo can significantly affect the radiation balance. Note that as vegetation cover is reduced in the late monsoon 2004 (Figure 2a), the albedo of the land surface begins to increase once again to reflect the drier, desert conditions.

Along with changes in albedo, vegetation greening leads to significant variations in the partitioning of surface turbulent fluxes, as captured by the evaporative fraction, $EF = \lambda E / (\lambda E + H)$, where H and λE are the daily-averaged sensible and latent heat fluxes. This is most clearly observed in monsoon 2007 (Figure 2c) where the measurements span the monsoon onset and vegetation response. Note the low values of *EF* (near zero), implying higher sensible heat fluxes, prior to the *NDVI* increase, and the dramatic increase in *EF* (~0.7 to 0.9) as available soil moisture from precipitation pulses is transferred back to the atmosphere via evapotranspiration. During each summer, individual storm events lead to increases in *EF* (e.g., higher latent heat flux) that are sustained over periods of several days. Interestingly, for periods with consecutive storms (low interstorm duration), sustained *EF* at high values may last for several weeks, for example in monsoon 2006 (Figure 2c). During the monsoon demise, vegetation becomes senescent and the *EF* decreases toward low values (see latter part of monsoon 2004, Figure 2a), implying a return to high sensible heat fluxes at the land surface.

Footprint-Averaged Hydrologic Conditions

In an effort to understand land-atmosphere interactions, we conducted a set of intensive surface measurements in the tower footprint (Figure 1a). For simplicity, we defined the footprint as 250-m by 250-m box around the tower, while recognizing that the actual measurement footprint will vary with wind conditions. For our purposes, this definition allows comparison of the estimated surface conditions to remotely-sensed observations from MODIS. As shown in Figure 1a, the topographic conditions around the tower are fairly uniform, as determined from a satellite-derived digital elevation model. Nevertheless, terrain variability at the site does include two stream channels, which have more abundant riparian vegetation as compared to exposed hillslopes at the site. As a result, we expected to capture spatiotemporal variations in soil temperature and moisture through daily sampling at the thirty (30) sampling plots in the tower footprint. Each sampling plot (~1m by 1m) was sampled at similar times each day during two week intervals in July and August 2006 and 2007. Measurements were performed using portable sensors, as described more fully in Vivoni et al. (2007).

Figure 3 (page 17) presents a comparison between the footprint-averaged, daily soil moisture (blue circles) and temperature (red triangles) conditions and the estimated daily Bowen Ratio ($B = H/\lambda E$, black circles). Surface fluxes and footprint hydrologic conditions are presented for monsoon 2006 (July 5 to 20, Figure 3a) and monsoon 2007 (July 19 to August 4, Figure 3b). The soil moisture and temperature symbols represent the average of the 30 plots, while the bars capture the spatial variability as ±1 std. The daily precipitation (bars) is included for reference. Note the good correspondence between the soil moisture and soil temperature and their relation to storm and interstorm periods. As expected, precipitation pulses promote a decrease in soil temperature and an increase in soil moisture, with consecutive storms leading to sustained wet and cool surface conditions. Interestingly, the spatial variability in the footprint is different in the two years, with monsoon 2007 exhibiting smaller spatial

variations in soil moisture and temperature, due to the effects of sustained cloud cover on limiting incoming solar radiation.

Of particular relevance is the relation between land surface conditions and the Bowen Ratio measured during monsoons 2006 and 2007. Note the excellent correspondence between footprint-averaged soil moisture and *B*, where periods of high *B* (large *H*) occur during interstorm periods, with rapid decreases in B (high λE) after precipitation pulses wet the land surface. Further analysis of the relation between B and footprint-averaged soil moisture (not shown) indicates that a power law behavior is observed for both monsoon seasons: $B = 4.95 \langle\theta\rangle^{-0.95}$ ($R^2 = 0.6$), where $\langle\theta\rangle$ is the footprint-averaged, daily soil moisture (%). This relation is significantly weakened when using the soil moisture conditions at the sampling plot near the tower. This suggests that the surface flux measurements are directly linked to the averaged soil moisture conditions in the tower footprint. Analysis comparing the tower and footprint-averaged conditions also revealed that the region around the tower is wetter and cooler than the tower plot, on average, for the two sampling periods.

Soil Moisture Controls on Evapotranspiration

The relation between surface fluxes and soil moisture conditions is particularly important as it forms an important parameterization in many land surface models (e.g. Vivoni et al., 2005). Typically, actual evapotranspiration (*ET*) is regulated by the amount of soil moisture present in the root zone, following a functional form that recognizes soil moisture limitations on *ET* below a threshold value (Rodríguez-Iturbe and Porporato, 2004). The functional form varies across different land surface models, but is generally assumed to be constant in time, with appropriate parameters selected for the ecosystem of interest. Unfortunately, few studies have attempted to establish the appropriate relationships between *ET* and soil moisture in ecosystems experiencing monsoonal greening and pulsed precipitation. As a result, most hydrological and climate models operating in the NAM region do not adequately capture vegetation dynamics in the parameterization of surface fluxes.

Figure 4 (Page 17) provides initial evidence for the temporal (and vegetation-dependent) variation of the relation between *ET* and soil moisture in the subtropical scrubland. Daily estimates of latent heat flux (λE), consisting of both evaporation and transpiration, are plotted as a function of the daily-averaged soil moisture from the tower sensor (at 5-cm depth, θ in vol. %) in Figure 4a. We use the tower site data due to the longer period of coincident measurements. Note the differences in the relation between λE and θ for each monsoon, suggesting the functional form may have interannual variations that depend on the vegetation state. For example, monsoon 2004 exhibits a maximum λE that asymptotes for high soil moisture values (~12 to 15 %) at ~4 MJ/day, while monsoon 2006 shows a maximum λE of nearly 12 MJ/day for soil moisture values of 10 to 12%.

Inspection of the *NDVI* time series for each monsoon season (Figure 4b), indicates that the sequence of $\lambda E(\theta)$ relations follows a similar order to that observed in the maximum *NDVI*. Monsoon 2006, which exhibited the higher values of λE for a given θ, also shows the highest vegetation greenness. This suggests that the subtropical scrubland at the EC tower site has a greater transpiration capacity during years with increased biomass resulting from above-average precipitation. As a result, the soil moisture control on *ET* varies temporally according to the ecosystem state.

Discussion and Conclusions

The evidence presented here on the interactions of surface fluxes and hydrological conditions in the North American monsoon region is based upon integrated, multiple-year studies at an eddy covariance tower site in the subtropical scrubland of northern Sonora, Mexico. The use of remote sensing data, EC tower observations and footprint measurements of surface conditions have revealed that: (1) the onset of the NAM leads to dramatic changes in surface properties and the partitioning of energy fluxes; (2) footprint-averaged soil moisture and temperature conditions are closely related to the surface fluxes; and (3) considerable variations exist between monsoon seasons, leading to vegetation-dependence on the relation between soil moisture and *ET*. On-going and future efforts in the study region include a detailed *ET* partitioning experiment based on the isotopic signature of water vapor, vegetation and soil samples (summer 2007); installation of a new EC tower site in the Río San Miguel (summer 2008); and land surface modeling using one-dimensional and distributed approaches to assess implications of our findings toward simulations and forecasts in the NAM region.

References

Douglas, M. W., Maddox, R. A., Howard, K., and S. Reyes, 1993: The Mexican monsoon. *J. Climate*, **6**, 1665-1677.

Gochis, D. J., Brito-Castillo, L., and W. J. Shuttleworth, 2006: Hydroclimatology of the North American monsoon region in northwest Mexico. *J. Hydrol*., **316**, 1-4, 53-70.

Rodríguez-Iturbe, I., and A. Porporato, 2004: Ecohydrology of water-controlled ecosystems: Soil moisture and plant dynamics. Cambridge University Press, 442 pp.

Salinas-Zavala, C. A., Douglas, A. V., and H. F. Díaz, 2002: Interannual variability of *NDVI* in northwest Mexico. Associated climatic mechanisms and ecological implications. *Remote Sens. Env.*, **82**, 2-3, 417-430.

Vivoni, E. R., Ivanov, V. Y., Bras, R. L., and D. Entekhabi, 2005: On the effects of triangulated terrain resolution on distributed hydrologic model response. *Hydrol. Process*., 19(11): 2101-2122.

Vivoni, E. R., Gutiérrez-Jurado, H. A., Aragón, C.A., Méndez-Barroso, L. A., Rinehart, A. J., Wyckoff, R. L., Rodríguez, J. C., Watts, C. J., Bolten, J. D., Lakshmi, V. and Jackson, T. J. 2007: Variation of hydrometeorological conditions along a topographic transect in northwestern Mexico during the North American monsoon. *J. Climate*, **20**(9), 1792-1809.

Watts, C. J., Scott, R. L., Garatuza-Payan, J., Rodríguez, J. C., Prueger, J. H., Kustas, W. P. and Douglas, M. 2007: Changes in vegetation condition and surface fluxes during NAME 2004. *J. Climate,* **20**(9), 1810-1820.

Zhu, C., Lettenmaier, D. P., and T. Cavazos, 2005: Role of antecedent land surface conditions on North American monsoon rainfall variability. *J. Climate*, **18,** 3104-3121.

From Higgins et al., page 9: Relationships between Gulf of California moisture surges and tropical cyclones in the Eastern Pacific Basin

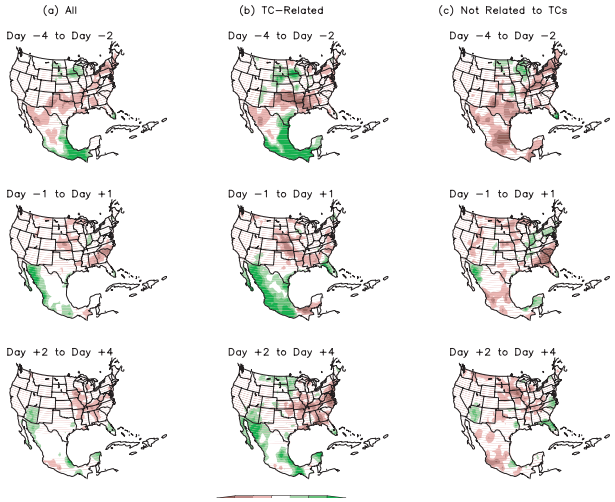

Figure 1. Composite evolution of accumulated precipitation anomalies (mm) for (a) all surges, (b) TC-related surges and (c) surges not related to TCs. Surges are keyed to Yuma, AZ. Day 0 is the onset date of the surges at Yuma. The accumulation period relative to onset is indicated on each panel. The shading interval is 1 mm day^{-1}and values greater than 1 mm day^{-1} (less than -1 mm day^{-1}) are shaded dark (light). The number of cases in each composite is given in Table 1, page 9.

From Rowe et al., page 12: Radar-based studies of convection in NAME

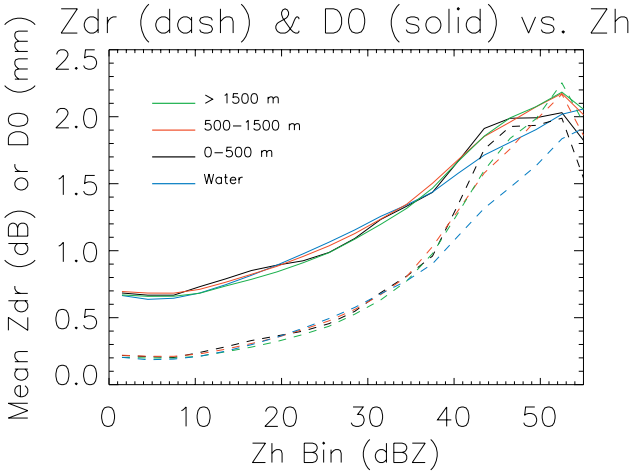

Figure 2. Near-surface differential reflectivity (ZDR) and median drop diameter (D0) as functions of reflectivity (ZH) for four terrain bands: over water, land 0-500 m, 500-1500 m, and 1500+ m MSL. Data from S-Pol during the NAME deployment (8 July-21 August 2004).

From Kursinski et al, Page 14: GPS observations of precipitable water and implications for the predictability of precipitation during the North American Monsoon

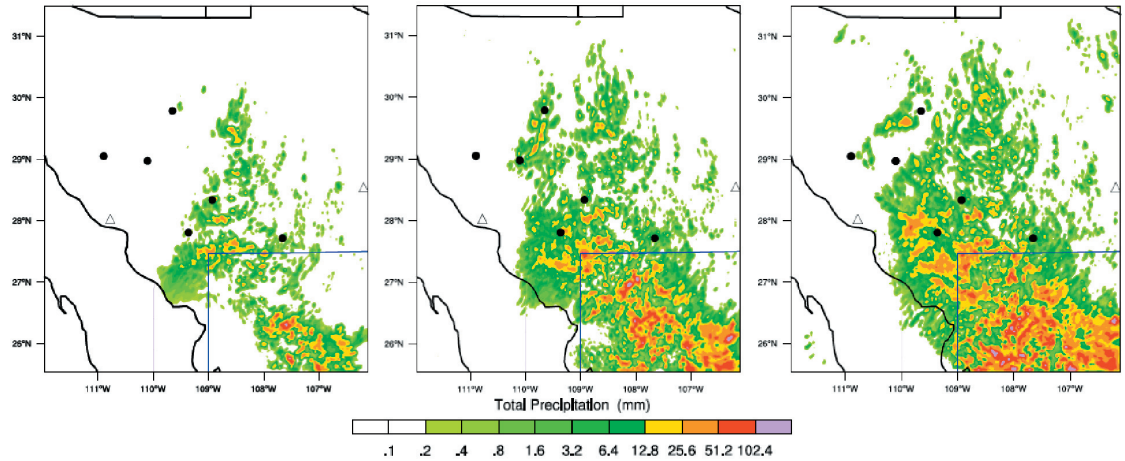

Figure 1. WRF simulations of accumulated precipitation for three different initial PWV fields, 95%, 100% and 105% of the ETA analysis PWV for July 29, 2004. Black dots indicate the locations of our GPS receivers. Triangles indicate the Empalme and Chihuahua radiosonde locations. Precipitation statistics in Figure 2 were derived in the southeastern region enclosed by the thin blue line.

From Vivoni et al, page 21: Relation between Surface Flux Measurements and Hydrologic Conditions in a subtropical scrubland during the North American Monsoon

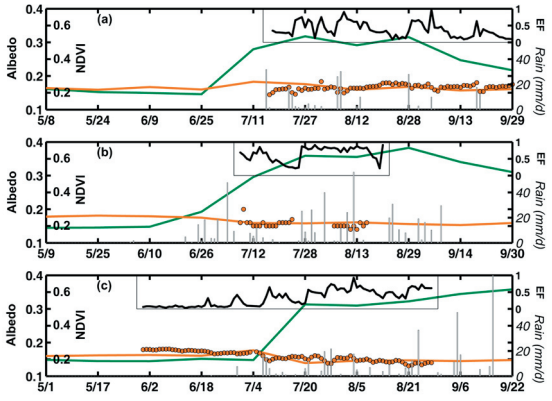

Figure 2. Seasonal evolution and interannual variability of rainfall, surface fluxes and land surface conditions at the EC tower for three monsoons: (a) 2004, (b) 2006, and (c) 2007. Rainfall (mm/day) is obtained from a tipping bucket rain gauge (gray bars). The MODIS sensor used to derive NDVI (green solid line) and albedo (orange solid line). MODIS albedo is compared to daily estimates at the EC tower obtained as the ratio of outgoing to incoming shortwave radiation ($a = R_{sout}/R_{sin}$, orange circles). Daily estimates of surface turbulent fluxes (sensible heat, H and latent heat, λE) are used to compute the evaporative fraction, $EF = \lambda E / (\lambda E + H)$, black solid line.

From Vivoni et al, page 21: Relation between Surface Flux Measurements and Hydrologic Conditions in a subtropical scrubland during the North American Monsoon

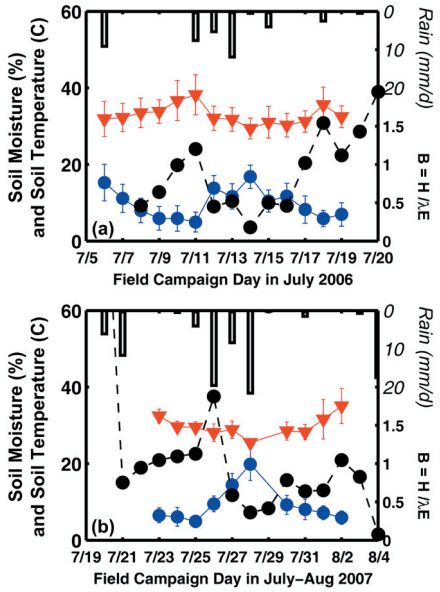

Figure 3. Footprint-averaged daily volumetric soil moisture (%, blue circles), surface soil temperature (°C, red triangles) and Bowen ratio (B = H / λE, black circles) estimated from the EC tower for (a) 2006 and (b) 2007. Footprint-averaging considers all 30 plots in 250-m by 250-m pixel around tower (symbol is spatial average and bars represent ±1 standard deviation). Daily rainfall (mm/day) from the tower site (bars) shown as reference.

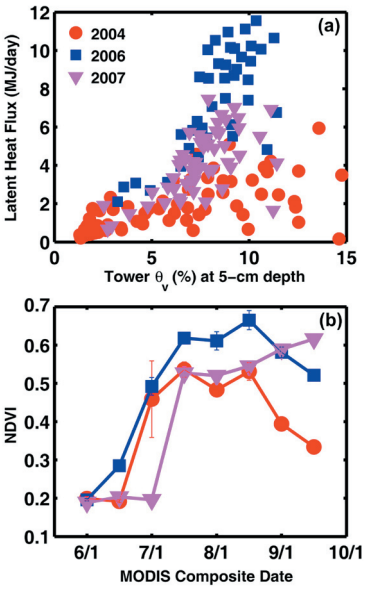

Figure 4. (a) Relation between daily latent heat flux (λE in MJ/day) and daily-average soil moisture (θ_v in %) obtained from a 5-cm depth sensor for 2004 (JD 205 to 275), 2006 (JD 189 to 228), and 2007 (JD 186 to 240). (b) Temporal evolution of NDVI from MODIS for 2004, 2006 and 2007, including spatial average of nine surrounding pixels (symbols) and ±1 standard deviation (bars).

From Munoz-Arriola et al., page 24: Extended West-wide Seasonal Hydrological System: Seasonal Hydrological Prediction in the NAMS region

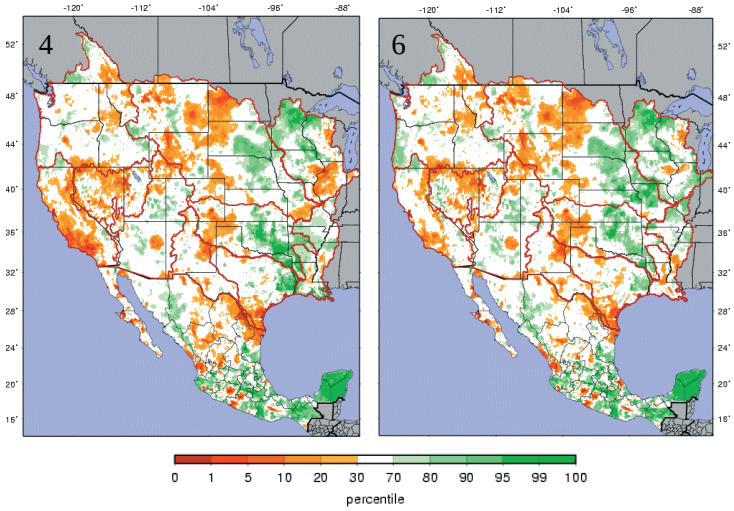

Figure 1. Soil Moisture Percentiles with respect to the 1960-1999 climatology for a) January 1st 2008 and b) January 15th 2008.

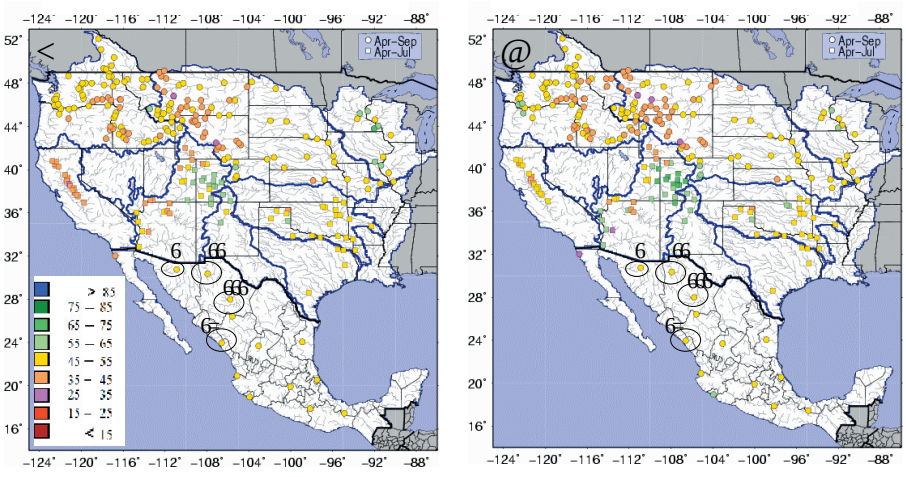

Figure 2. Forecasts effective 1/1/08 (a) and 1/15/08 (b) as streamflow percentiles for the western United States and Mexico for the period April-September (circles) and April-July (squares), 2008. Dots indicated percentiles relative to the 1960-1999 climatology. Circled points show locations of stations in the NAMS core region: I) Imuris, II) Casas Grandes, III) Conchos,and IV) Ixpalino.